Correlating the Resisting Mechanisms and the Strength of Thin Shells Under Follower Loads

Bulletin of Osaka Prefecture University
Series A, Vol. 45, No. 2, 1996, pp. 87-97

Correlating the Resisting Mechanisms and the Strength of Thin Shells under Follower Loads

Thomas GEORGE* and Hiroo OKADA*

(Received November 29, 1996)

This paper deals with the internal mechanisms of resisting an external follower load and the elastic strength limits of thin shells. Owing to their form resistance, shells are inherently advantaged to function under very high loading requirements, where the strength and stability are the primary concerns.

A set of governing equations for thin shells defined in a system of monoclinically convected coordinate axes are used for this analysis. The resisting mechanisms of a shell are derived from different components of terms associated either with the extensional or the bending stiffness parameters. The physical nature of equilibrating the governing equation is studied here by numerically analyzing the share of contributions from these different components. Also, an analysis of the stress resultants at selected points of the shell geometry during large deformations brings out the development of severely stressed zones during the deformation process, and thus provides a realistic picture of possible local elastic failure points.

Finally, the numerical results for the resisting mechanisms and strength characteristics are brought together and their underlying features are analyzed with the comparative measures of shell stability. As a result, some general characteristics of both singly and doubly curved partial shells are established. These results are promising to the extend of explaining some of the instability mechanisms exhibited by thin shells during finite deformations.

1. Introduction

The allowable tolerance for structural systems are statistically estimated during the design stage within the scope of known or predictable loading conditions. It becomes one of primary importance to make the closet possible estimate of the strength of any structure before placing it to an operation field with unpredictable conditions. Shells are very prone to have some uncertain design criteria due to the mostly unavailable details of their stability or strength characteristics, as compared to other components of a structure.

The theory of shells by itself is a well researched subject and numerous studies have been conducted on its advanced aspects[1-5]. However, the elastic stability analyses of shells are not necessarily accompanied by a study of the strength aspects, which in fact is taken for granted in most situations[6-8]. This paper deals exclusively with a comparative study of the resisting mechanisms and the elastic strength of thin shells subjected to follower loads.

*Department of Marine System Engineering, College of Engineering

The governing equations for thin shells were derived here in a system of monoclinically convected coordinate axes defined over the middle surface. The systematic presentation of tensor derivations from the first principles of continuum mechanics, and other details of that derivation have been the subject of study in many of the previous papers[5,6]. Those analytic equations were derived with proper consideration of the shell geometry after deformation, which was expected to make the numerical results to be more exact than a formulation based on the pre-deformation metric and curvature values. The ability of this formulation to deal with the large deformations and the stability mechanisms of several types of thin shells have also been verified in some of the earlier studies[6,7].

The internal resisting mechanism of thin shells can be considered as derived either from the extensional or the bending stiffness. These resisting factors are qualitatively divided into different groups of terms, each of which contributes in varying proportions to the total resisting mechanism of the shell at its deformed states. Also, the elastic stresses developed in the shell vary across the shell thickness at different points, some of which would attain the limit states even before the static failure points. Here, the stress resultants

were calculated at selected points of the shell geometry using the physical components of the normal and tangential stresses due to the membrane forces and the moments.

The detailed aspects of the resisting mechanism and the elastic strength were independently analyzed in different studies, which would be correlated in this paper to bring out the comparative characteristics. Partial cylindrical and spherical shells with curvatures ranging from very shallow to very deep were considered here. These analyses have brought out a pattern of resistance mechanism and strength characteristics, and established some critical curvature ranges of shells for which the elastic strength might be lower than the plate strength, though mostly a local effect for shells.

The Galerkin method was used for numerical formulations, for a specific simply supported boundary condition only. Attempts for generalizations were therefore restricted to the partial cylindrical and spherical shells, which might be extended safely to other types of shells and different loading and boundary conditions, gererally for their qualitative aspects.

2. Theoretical Formulations

The general governing equations for a thin shell are formulated here in the *monoclinically convected coordinate axes* (θ^1, θ^2, θ^3) traced over the shell middle surface, where the θ^3 direction is adopted normal to that surface, as shown in Fig. 1.

The *Kirchhoff-Love* assumptions are assumed true throughout the finite deformation process of a thin shell. The *Range Convention* adopted here for indices

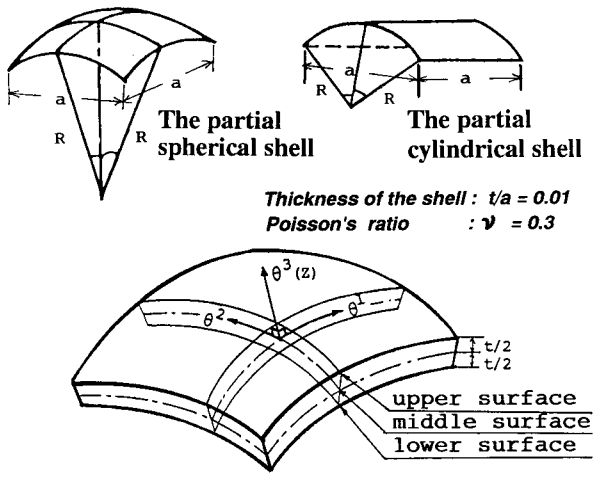

Fig.1 The definition of monoclinically convected coordinate axes and the geometry of two particular shell types

is such that all *Latin* indices ($i, j, k, \cdots$) take values 1, 2, 3 and all *Greek* indices ($\alpha, \beta, \gamma, \cdots$) have the range 1, 2. Various other notations and symbols used in this paper will be explained when and where they appear first.

2.1 Fundamental Equations

The general surface strain of the shell is expressed here using the 2-dimensional form of the *Green-Lagrange* strain tensor, and its middle surface counterpart $\varepsilon_{\alpha\beta}$ may be defined in terms of the corresponding metric tensors before deformation ($a_{\alpha\beta}$) and after deformation ($A_{\alpha\beta}$) of the middle surface.

$$\left.\begin{aligned} \varepsilon_{\alpha\beta} &= \frac{1}{2}(A_{\alpha\beta}-a_{\alpha\beta}) \\ A_{\alpha\beta} &= a_{\alpha\beta}+u_\alpha|_\beta+u_\beta|_\alpha+u^i|_\alpha\ u_i|_\beta \end{aligned}\right\} \quad (1)$$

The metric tensors can be derived directly from the first principles using the position vectors before and after the deformation of any point on the middle surface and the corresponding deformation vector. The symbol ' | ' denotes 3-dimensional (*spacial*) covariant differentiation with respect the subscript that follows, as different from its 2-dimensional (*surface*) counterpart ' ‖ ' which will be used later.

Also, the curvature tensor of the middle surface after deformation $B_{\alpha\beta}$ may be expressed as the sum of the curvature tensor before deformation $b_{\alpha\beta}$ and the change of curvature tensor $\varkappa_{\alpha\beta}$.

$$\left.\begin{aligned} B_{\alpha\beta} &= b_{\alpha\beta}+\varkappa_{\alpha\beta} \\ \varkappa_{\alpha\beta} &= u^3|_{\alpha\beta}-u^3|_\gamma\ u^\gamma|_{\alpha\beta} \\ &\quad +\frac{1}{2}(u^\gamma|_\gamma u^\delta|_\delta-u^\gamma|_\delta u^\delta|_\gamma-a^{\gamma\delta}u^i|_\gamma u_i|_\delta)b_{\alpha\beta} \end{aligned}\right\} \quad (2)$$

The *Cauchy* stress tensor $\sigma^{\alpha\beta}$ for isotropic materials is used here in its 2-dimensional form to express the stress-strain relationship on the general surface, where E is the Young's Modulus of elasticity and ν is the Poisson's Ratio.

$$\sigma^{\alpha\beta}=\left(\frac{E}{1-\nu^2}\right)G^{\alpha\beta\gamma\delta}\eta_{\gamma\delta} \quad (3)$$

The quantity $G^{\alpha\beta\gamma\delta}$ is a fourth order tensor known as the 'Elasticity Tensor' for the general surface, which may be expressed in terms of its middle surface counterpart $A^{\alpha\beta\gamma\delta}$ using appropriate *shifter* parameters for contravariant quantities after deformation.

The membrane force tensor $N^{\alpha\beta}$ and the moment tensor $M^{\alpha\beta}$ may be derived through the direct integration of stress components across the shell thickness t. After proper substitutions and reductions, the membrane force and moment tensors can be expressed completely in terms of the middle surface quantities.

$$N^{\alpha\beta}=Da^{\alpha\beta\delta\lambda}\varepsilon_{\delta\lambda}+Ka^{\varepsilon\beta\eta\xi}(b^{\phi}_{\phi}\delta^{\alpha}_{\varepsilon}\delta^{\delta}_{\eta}\delta^{\lambda}_{\xi} - b^{\alpha}_{\varepsilon}\delta^{\delta}_{\eta}\delta^{\lambda}_{\xi}-b^{\lambda}_{\xi}\delta^{\alpha}_{\varepsilon}\delta^{\delta}_{\eta})\kappa_{\delta\lambda} \quad (4)$$

$$M^{\alpha\beta}=Ka^{\alpha\beta\delta\lambda}\kappa_{\delta\lambda}+Ka^{\varepsilon\beta\delta\lambda}(b^{\phi}_{\phi}\delta^{\alpha}_{\varepsilon}-b^{\alpha}_{\varepsilon})\varepsilon_{\delta\lambda} \quad (5)$$

In the above equations, D and K are respectively the *extensional stiffness* and the *bending stiffness* parameters, $\delta^{\alpha}_{\varepsilon}$ is the Kronecker delta and $a^{\alpha\beta\gamma\delta}$ is the elasticity tensor of the middle surface before deformation, as given below.

$$D=\frac{Et}{(1-\nu^2)}\ ,\quad K=\frac{Et^3}{12(1-\nu^2)} \quad (6)$$

$$a^{\alpha\beta\gamma\delta}=\left(\frac{1-\nu}{2}\right)[a^{\alpha\gamma}a^{\beta\delta}+a^{\alpha\delta}a^{\beta\gamma}]+\nu a^{\alpha\beta}a^{\gamma\delta} \quad (7)$$

The above expressions for membrane force and moment tensors are simplified for small deformations. However, the middle surface curvature before deformation (b^{α}_{β}) may be replaced by the corresponding value after deformation (B^{α}_{β}) for the general case of finite deformations.

Now, the transverse shear force can be eliminated by substitutions from the equilibrium equations of a thin shell, whereby the following governing equations can be formulated for finite deformations.

$$N^{\alpha\beta}\underset{(a)}{\|}_{\alpha}+M^{\alpha\gamma}\underset{(a)}{\|}_{\alpha}B^{\beta}_{\gamma}=-p^{\beta}-m^{\alpha}B^{\beta}_{\alpha} \quad (8)$$

$$N^{\alpha\beta}B_{\alpha\beta}-M^{\alpha\beta}\underset{(a)}{\|}_{\alpha\beta}=-p^{3}+m^{\alpha}\underset{(a)}{\|}_{\alpha} \quad (9)$$

Here the quantity m^{α} is the sum of the surface tractions and body forces contributed moment load, p^{β} and p^{3} are respectively the tangential and normal components of the applied load. The symbol (a) below the 2-dimensional (*surface*) covariant differentiation sign '$\|$' denotes differentiations performed on quantities after deformation.

For analytical simplifications, the middle surface strain and the change of curvature tensors may be expressed in their partial differential forms, as given below.

$$\left.\begin{aligned}\varepsilon_{\alpha\beta}&=\frac{1}{2}\{u_{\alpha,\beta}+u_{\beta,\alpha}-2(b_{\alpha\beta}u_3+\Gamma^{\lambda}_{\alpha\beta}u_{\lambda})+b^{\lambda}_{\alpha}b_{\lambda\beta}(u_3)^2\\&\quad+u_{3,\alpha}u_{3,\beta}+b^{\lambda}_{\alpha}[(b^{\rho}_{\beta}u_{\rho}+u_{3,\beta})u_{\lambda}\\&\quad+(\Gamma^{\rho}_{\lambda\beta}u_{\rho}-u_{\lambda,\beta})u_3]+b^{\lambda}_{\beta}(u_{\lambda}u_{3,\alpha}-u_{\lambda,\alpha}u_3)\}\\\kappa_{\alpha\beta}&=u_{3,\alpha\beta}-b^{\lambda}_{\alpha}b_{\beta\lambda}u_3-\Gamma^{\lambda}_{\alpha\beta}u_{3,\lambda}+(b^{\lambda}_{\beta}u_{3,\alpha}+b^{\lambda}_{\alpha}u_{3,\beta})u_{3,\lambda}\\&\quad+\frac{1}{2}[b^{\lambda}_{\lambda}b^{\rho}_{\rho}(u_3)^2-b^{\lambda}_{\rho}b^{\rho}_{\lambda}(u_3)^2]\,b_{\alpha\beta}\end{aligned}\right\} \quad (10)$$

$\Gamma^{\lambda}_{\alpha\beta}$ are the *Christoffel symbols* and u^k or u_k ($k=1, 2, 3$) represent the covariant and contravariant deflection components in the three coordinate directions. The deflection components can be considered here in the form of an algebraic summation series, as follows:

$$u_k=\sum_{i=1}^{m}\sum_{j=1}^{n}U_{k(i,j)}\phi_k(\theta^1,\ \theta^2) \quad (11)$$

Here, U_k represent the deflection coefficient and $\phi_k(\theta^1, \theta^2)$ may be considered as a double trigonometric function, where θ^1 and θ^2 are the angular coordinates of the middle surface in the principal directions.

2.2 Equations for the Resisting Mechanism

This paper considers the resisting mechanism during the normal deformations of a thin shell. Eq. (9) which is the governing equation in the normal direction is to be analyzed here in detail to bring out the contributions to the total resisting mechanism by each component term.

The equilibrium in the normal direction may be represented in the following form where the $\mathcal{E}$ term denotes the group of terms that club together with the *Extensional stiffness parameter* D and the $\mathcal{B}$ term denotes the group of terms that club together with the *Bending stiffness parameter* K.

$$\mathcal{E}+\mathcal{B}=-p^3 \quad (12)$$

Now, the terms $\mathcal{E}$ and $\mathcal{B}$ may be subdivided into the following components, where the **E** terms and the **B** terms denote a division based on the characteristics of each group of terms.

$$\left.\begin{aligned}\mathcal{E}&=\mathbf{E1}+\mathbf{E2}+\mathbf{E3}+\mathbf{E4}\\\mathcal{B}&=\mathbf{B1}+\mathbf{B2}+\mathbf{B3}+\mathbf{B4}\end{aligned}\right\} \quad (13)$$

The significance and meaning of this arbitrary subdivision is visible when each group of terms is studied from the following detailed representation of their component structures.

$$\left.\begin{aligned}\mathbf{E1}&=D(a^{11})^2\varepsilon_{11}B_{11}\\\mathbf{E2}&=D\nu a^{11}a^{22}[\varepsilon_{11}B_{22}+\varepsilon_{22}B_{11}]\\\mathbf{E3}&=D\left(\frac{1-\nu}{2}\right)a^{11}a^{22}[(\varepsilon_{12}+\varepsilon_{21})(B_{12}+B_{21})]\\\mathbf{E4}&=D(a^{22})^2\varepsilon_{22}B_{22}\end{aligned}\right\} \quad (14)$$

$$\left.\begin{aligned}\mathbf{B1}&=K(a^{11})^2[\kappa_{11}B_{11}(b^2_2-b^1_1)-\kappa_{11,11}-\varepsilon_{11,11}b^2_2]\\\mathbf{B2}&=-K\nu a^{11}a^{22}[\kappa_{11,22}+\kappa_{22,11}+\varepsilon_{11,22}b^1_1+\varepsilon_{22,11}b^2_2]\\\mathbf{B3}&=-K\left(\frac{1-\nu}{2}\right)a^{11}a^{22}[2(\kappa_{12,12}+\kappa_{21,12})\\&\quad+(\varepsilon_{12,12}+\varepsilon_{21,12})(b^1_1+b^2_2)]\\\mathbf{B4}&=K(a^{22})^2[\kappa_{22}B_{22}(b^1_1-b^2_2)-\kappa_{22,22}-\varepsilon_{22,22}b^1_1]\end{aligned}\right\} \quad (15)$$

For the sake of convenience and easy visualization

effect, the above equations are given in terms of strain components, curvatures and the change of curvature. First all, the terms **E1** and **B1** contain terms grouped together with the metric tensor in the first principal direction θ^1 (the term 'primary direction' will be used in further discourse) and the terms **E4** and **B4** contain terms grouped together with the metric tensor in the second principal direction θ^2 (the term 'secondary direction' will be used in further discourse). The terms **E1** and **E4** represent the stretch in the respective principal directions, whereas the terms **B1** and **B4** represent the bending in the respective principal directions.

Next, the terms **E2**, **E3**, **B2** and **B3** are groups of terms accompanying the product of metric tensors in the principal directions and characterized by the presence of the Poisson effect. They are basically the cross components of stretching and bending in the principal directions. The difference lies in the fact that the terms **E2** and **B2** represent the effects due to strains and curvatures or its changes in the principal directions, whereas the terms **E3** and **B3** are associated with the shear and twist components.

The terms $\mathcal{E}$ and $\mathcal{B}$ will be denoted in further discourse as the **Extensional part** and the **Bending part**, respectively. Also, their subdivisions will be denoted as the **Component terms**. The above notations are to be followed for all the evaluations made on the resisting mechanisms of thin shells during the numerical analyses conducted in this paper.

2.3 Equations for Strength Calculations

The tensor components for stress resultants as calculated above, may be physically interpreted using the following conversion scheme[2,5], where the quantities with bracketed subscripts denote the physical components. It should be specially noted that the *Einstein's Summation Convention* is not applicable for the identical repeated indices in these equations.

$$\left.\begin{aligned} N_{(\alpha\beta)} &= N^{\alpha\beta}\sqrt{\frac{A_{\alpha\alpha}}{A^{\beta\beta}}} \\ M_{(\alpha\beta)} &= M^{\alpha\beta}\sqrt{\frac{A_{\alpha\alpha}}{A^{\beta\beta}}} \end{aligned}\right\} \tag{16}$$

Also, the physical (actual) stress components in the normal and tangential (shear) directions may be calculated using either one of the following equations[1,2].

$$\sigma_{(\alpha\beta)} = \sigma^{\alpha\beta}\sqrt{\frac{G_{\alpha\alpha}}{G^{\beta\beta}}} \tag{17}$$

$$\sigma_{(\alpha\beta)} = \frac{N_{(\alpha\beta)}}{t} - \frac{12M_{(\alpha\beta)}z}{t^3} \tag{18}$$

The quantities $G_{\alpha\alpha}$ and $G^{\beta\beta}$ are the metric tensors of the general surface after deformation, which may be calculated from the corresponding values of the middle surface using appropriate *shifter* parameters for transformations between the two surfaces[5].

In this paper, the direct stress and the bending stress are calculated correspondingly by the $N_{(\alpha\beta)}$ and $M_{(\alpha\beta)}$ terms in Eq. (18). There would arise a small difference, which is negligible for all practical purposes, between the stresses calculated using the above two equations. This is mainly due to the differences in the extent of simplifications during the stages of reductions leading to these equations, and to some extent due to the assumption of linear stress distributions across the shell thickness[1] adopted in Eq.(18).

3. Numerical Analyses of the Resisting Mechanism and Strength

The most important problems accompanying shell designs are the many unknown characteristics that the shell might display at the large deformation stage. In the numerical analyses conducted in this research, two of such characteristics, the resisting mechanisms and the strength, are studied thoroughly. The shell theory was described briefly in **ch. 2** for the general thin shell continuum and two of the major shell types, partial cylindrical and partial spherical shells, are chosen to represent the singly curved (zero Gaussian curvature) and doubly curved (positive Gaussian curvature) shells.

The shell boundaries are considered simply supported, with all the inplane deflections arrested along the edges. A uniformly distributed pressure load is considered to be acting in the anti-radial direction, and the letter **p** ($=|p^3|$) is used in the graphical representations of results. The shell geometry is considered to be that which produces a projected square base of unit area, by which the principal chord lengths $[a=l_1=l_2]$ are unity. In order to satisfy the fundamental assumptions, the shell thickness t, which is considered uniform, is assumed to be sufficiently small $[t/a=0.01]$ in comparison with the radius R. The numerical value

of $E=1.96\times10^{11}$ N/m^2 for the *Young's modulus* and the *poisson's ratio* of $\nu=0.3$ are used in the numerical calculations.

The differential geometry of a toroidal shell is used to express the basic values on the middle surface. The corresponding equations for the metric and curvature tensors and the Christoffel symbols can easily be formulated from first principles[5]. The 'primary direction' (*see* **sec. 2.2**) of partial cylindrical shells in chosen in its longitudinal direction.

The equilibrium equations [Eqs. (8), (9)] under static considerations are solved using the Galerkin method, with 16 modal combinations. [m, $n=4$, in Eq. (11)] . Curvature ranges of shells are selected from the plate ($R/a=\infty$) to the subtended angle of π *radians* at the center ($R/a=0.5$) for the deep shell. Generally, all graphical representations of numerical results are nondimensionalized appropriately. Some details of the numerical results for the finite deformations and instability characteristics of different shells[6,7], the results of which are partly incorporated in this paper, are provided in an accompanying paper.

3.1 The Resisting Mechanism

In the numerical analysis to determine the resisting mechanism of shells using Eq. (12), instead of considering only a single monitoring point, for example the center of the shell, the average value of several symmetric mesh points is calculated. The term *average deflection* denotes the analytically integrated average of the deflection values u^3 over the whole surface. The allowable error in satisfying Eq. (12) is restricted well within 1.0% by adjusting the number of mesh points. About 40 different curvature values each for the partial cylindrical and spherical shells are numerically analyzed. The term *influence parameter* used in the graphical results indicates the fraction of influence shared by a component term in the total resisting mechanism of the equilibrium equation for deformations in the normal direction.

3.1.1 Initial Resisting Mechanism

The initial shares of extensional and bending stiffness parts are shown in Fig. 2. Shallow curvatures are shown towards the right where the bending part ($\mathcal{B}$) has complete domination, and at the left extreme where deep shells are shown, the extensional part ($\mathcal{E}$) dominates the resisting mechanism.

The curves for partial spherical shells are more shifted towards the shallow shell end than the partial

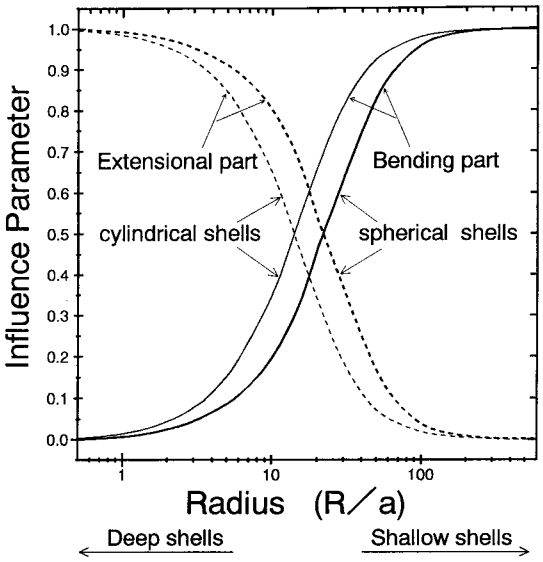

Fig.2 The share of extensional and bending stiffness parts in the initial resisting mechanisms of different shells

cylindrical shell, which is very much in accordance with the logical arguement that for doubly curved shells the effect of curvature appears at more shallow curvatures than singly curved shells for which the effect of bending in the primary direction lasts until deeper shells. More detailed analyses of the component parts can also show, among various other interesting details, that for deep cylindrical shells the extensional component in the radial direction **E4** is the sole contributor to its resisting mechanism.

3.1.2 Resisting Mechanism in Deformed States

The results for initial influences of various components are roughly representative of the deformed equilibriums also. However, the mechanism of deformation is accompanied by geometrical changes which initiate some considerable changes in the resisting mechanism of the shell. The total resisting mechanism is composed of several smaller terms that constitute each component term of Eq. (12). For a deeper understanding of the resisting mechanism, it might be worthwhile to study some of those terms in detail and determine their shares in the total resisting mechanism.

Fig. 3 and Fig. 4 show the variations in the influence of different terms in the total resisting mechanism during deformed states. The top row of 3 figures each shows the aggregate influence and the bottom row shows the influence due to component terms of the bending and the extensional parts. Figures (a-1) and (b-1) can be found to be of the same type for both shells except for the effects of unsymmetry of principal

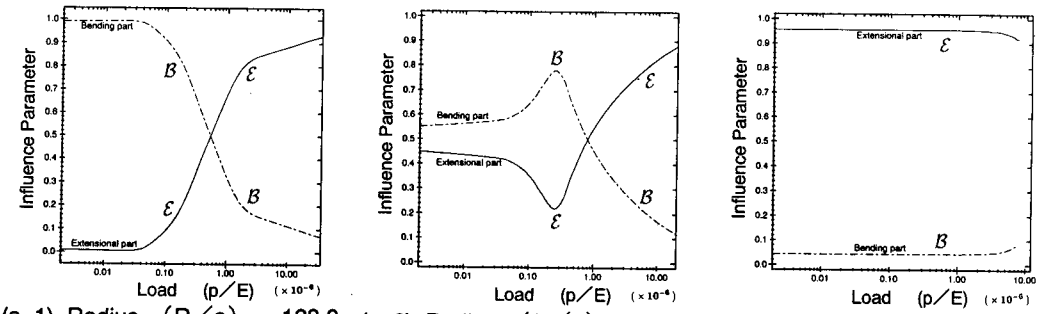

(a-1) Radius (R/a) = 128.0 (a-2) Radius (R/a) = 16.0 (a-3) Radius (R/a) = 2.0

(a) Aggregate influence

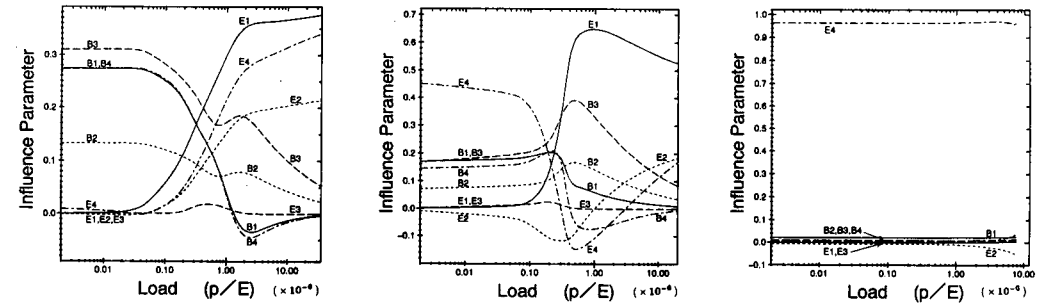

(b-1) Radius (R/a) = 128.0 (b-2) Radius (R/a) = 16.0 (b-3) Radius (R/a) = 2.0

(b) Influence of component terms

Fig.3 Variations in the share of different components in the resisting mechanisms of some partial cylindrical shells

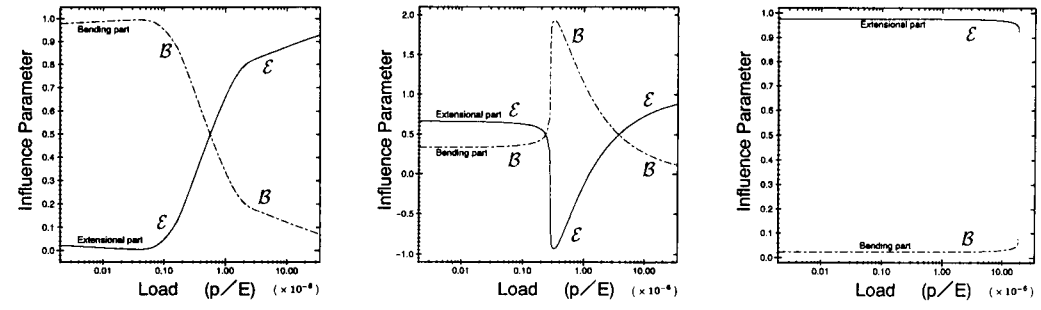

(a-1) Radius (R/a) = 128.0 (a-2) Radius (R/a) = 16.0 (a-3) Radius (R/a) = 2.0

(a) Aggregate influence

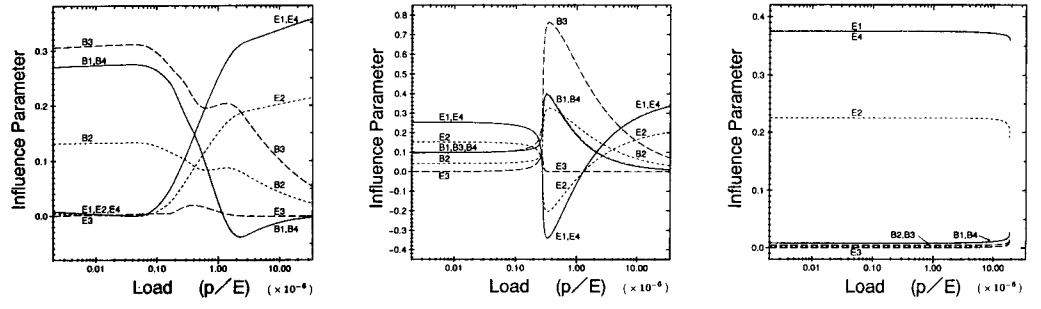

(b-1) Radius (R/a) = 128.0 (b-2) Radius (R/a) = 16.0 (b-3) Radius (R/a) = 2.0

(b) Influence of component terms

Fig.4 Variations in the share of different components in the resisting mechanisms of some partial spherical shells

directions in the case of the cylindrical shell. The domination of the bending components disappear at higher loading stages of shallow shells, which shows the importance of extensional terms for shallow shells also when considering large deformations.

In Figures (a-2) and (b-2), the resisting mechanisms do not match between the two shells. For cylindrical shells in Fig. 3 the initial domination is by the bending part for the presence of its primary direction, which is the other way in Fig. 4 for the spherical shells. However, at higher loading stages the dominant parts reverse for the cylindrical shell while the initially dominant part of the spherical shell regains the position after an intermediate reversal of roles. The details of this picture given in (b-2) for both shells in terms of the corresponding components show the extremely complicated influence changes occuring around the static instability point of each shell.

Figures (a-3) and (b-3) are much less complicated, where the extensional parts clearly dominate and their components follow the natural conclusions. It may be seen from the above illustrations that for both types of shells the curvatures may be broadly divided into an 'extension zone', a 'bending zone' and a 'combined zone' based on the resisting mechanisms. Deep shells in the 'extension zone' follow the evidently straightforward pattern, and for shells in the 'combined zone' extensional and bending parts demonstrate a very complicated role playing.

3.1.3 Characteristic Curves of the Resisting Mechanism

The resisting mechanisms of shells from the shallow to deep curvature ranges are calculated and the results are shown in Fig. 5 and Fig. 6. Here, the boundaries of influence zones for each component term is plotted as continuous lines, where the influence zones are measured as the range of influence parameters greater than 0.01 (1.0% share of the total influence or more). The 'Threshold of static instability' is determined based on the combined estimation using the results of an earlier study[6] on the natural frequencies of vibration of the deflected shell and the ultimate loading values from the present study. The resisting mechanism is calculated for loading stages within this threshold load only, since the mechanism undergoes many changes beyond this point.

As for the method of reading these graphs, the boundaries of influence zones for each component plotted here represents the appearance of that component when moving upwards through the direction of increasing load for each radius. A curve due to a component that does not appear at any loading stage can be considered to have its influence zones for all loading levels at that radius. Thus, at any radius the portion of an ordinate below the point of an intersection with a curve is the 'no influence zone' of load levels for that component.

In both figures, shallow shells towards the right end are dominated by bending terms $\mathcal{B}$ only, until a higher loading stage where the influence of the extensional part $\mathcal{E}$ appears. This can be understood easily by

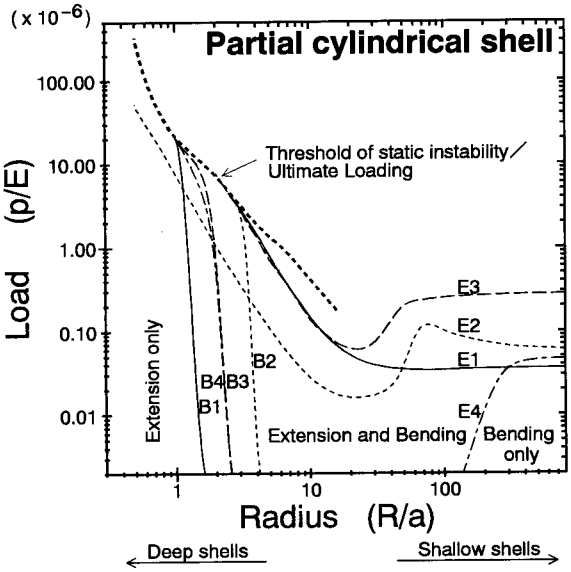

Fig.5 Influence zones of different components in the resisting mechanisms of partial cylindrical shells

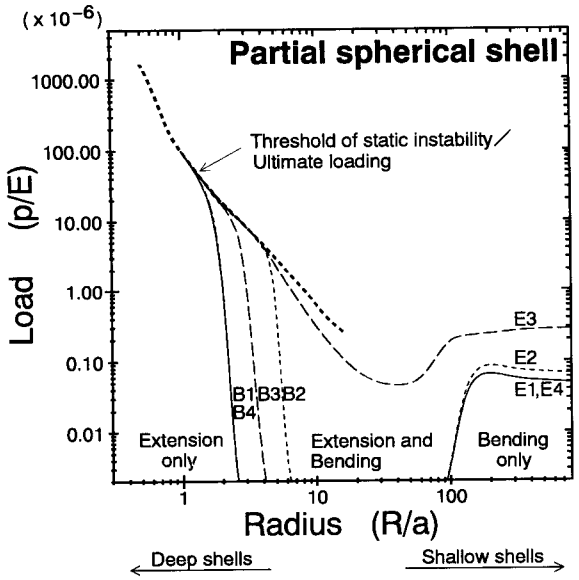

Fig.6 Influence zones of different components in the resisting mechanisms of partial spherical shells

considering that the deflected shell attains curvatures which bring in the extensional effect. Now, for deep shells towards the left end the picture is considerably different for cylindrical and spherical shells.

For the partial cylindrical shells shown in Fig. 5 the influence zones due to extensional components **E1**, **E2** and **E3** appear only at very high loading stages at or near the static instability. The initial influence zone at the deep shell end is completely dominated by the principal stretch component **E4** in the radial direction. However, for the partial spherical shells shown in Fig. 6 the only extensional component that does not appear during the lower loading stages is the inplane twist **E3** for the complete range of curvatures, and the principal stretch components **E1** and **E4** are symmetric for all curvatures.

The appearance of influence zones due to the bending components **B1** to **B4** in the case of both the shells can be seen starting after the 'extension only' zone and remains so for the whole range of shallower shells towards the right of the figure. In the case of cylindrical shells in Fig. 5 the principal bending component **B1** due to the primary direction appears first and the other components follow in suit at shallower curvatures as is expected.

The influence zone that appears in between the extremes is shared by both the extensional and the bending parts. The overall width of this zone is slightly larger for cylindrical shells due to the early appearance of the effect of bending at the deep shell side and the late disappearance of the effect of extension in the radial direction at the shallow shell end.

3.2 Strength Analysis

In the numerical analysis using Eq. (18) to determine the stress states of shells, instead of considering only a single point for monitoring the stress variations, for example the center of the shell, four different points on a quarter shell area are considered simultaneously. Fig. 7 shows the points chosen for monitoring, where point A is the center of a quarter shell ($\theta^1=0.25\,\Omega_1$, $\theta^2=0.25\,\Omega_2$), points B and C being the center points on the principal curvature lines intersecting at point A ($\theta^1=0.25\,\Omega_1$, $\theta^2=0.50\,\Omega_2$ and $\theta^1=0.50\,\Omega_1$, $\theta^2=0.25\,\Omega_2$ repectively), and point D is the center of the complete shell ($\theta^1=0.50\,\Omega_1$, $\theta^2=0.50\,\Omega_2$). Here, Ω_1 and Ω_2 are the subtended angles at the center of curvature in each principal direction.

About 25 different curvature values each for the partial cylindrical and spherical shells are used for this analysis. For an estimation of the *elastic limit stress* state, the yield point stress for the material (σ_y) is chosen as 300.0 MPa, and the value $(\sigma_{(\alpha\beta)}/\sigma_y)=1.0$ becomes the limit state of stress at the given monitoring point in the direction indicated.

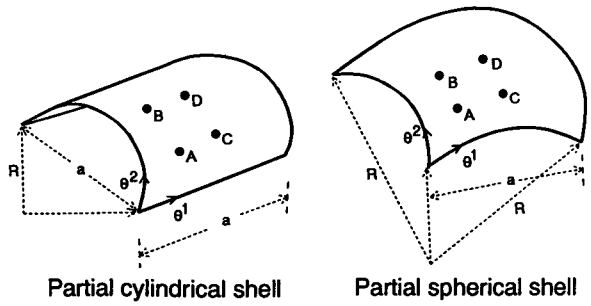

Fig.7 Monitoring points for stress calculations

3.2.1 Calculation of Stresses

As the shell undergoes deformations at subsequent loading states, the state of stress at each point undergoes variations, which could be associated either with the direct stresses due to the membrane force distributions or the bending stresses due to the moment distributions. The contributions from both sources could further be divided into normal stresses and tangential shear stresses.

In Eq. (18) direct stresses are given by the first term and bending stresses by the second. Further, normal stresses are calculated when $\alpha=\beta$ and tangential shear stresses are obtained when $\alpha\neq\beta$ in the subscripts within brackets. The assumption of linear distribution of all stresses across a shell cross section is considered valid here.

Fig. 8 (a) shows the variations of normal stresses at the monitoring point **A** of a typical shell (partial spherical shell, $R/a=2.0$). The vertical chain line in Fig. 8 (a) indicates the limit stress state on the upper surface **A(U)** in both θ^1 and θ^2 directions at the load level as given by the horizontal chain line. Fig. 8 (b) elaborates upon the stress levels at other monitoring points when the stress level **A(U)** reaches the limit stress state. This particular case is evidently that of a fully compression shell since all the monitoring points give compressive stresses only.

Generally, at the limit stress state for any one of the monitoring points, some shells have fully compressive stresses at all points whereas, some other shells have a compression and tension sharing situation or a tension dominated situation. Only normal stresses are shown

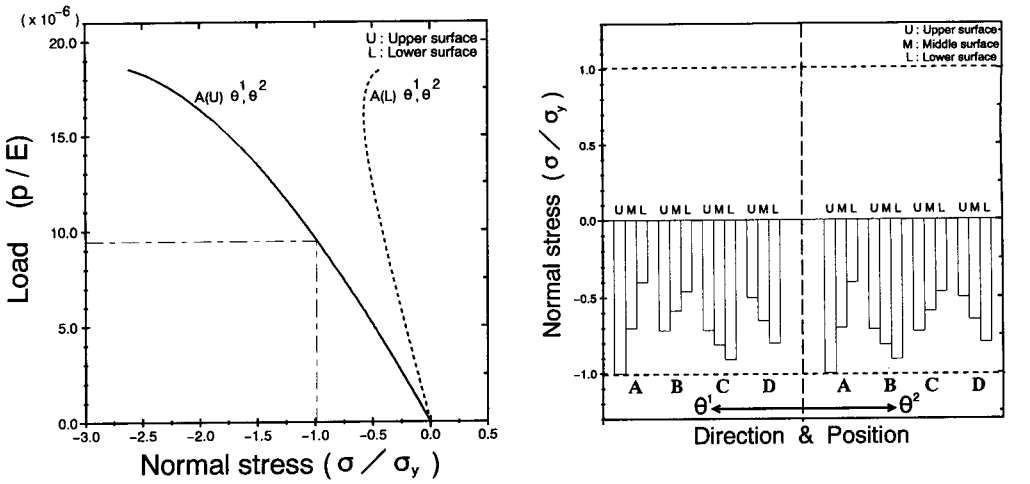

(a) Variation of Normal Stresses (b) Stress states for the Limit state

Fig.8 An example for the variation of normal stresses with load and the stress states at the monitoring points for the limit state (Partial spherical shell, $R/a=2.0$)

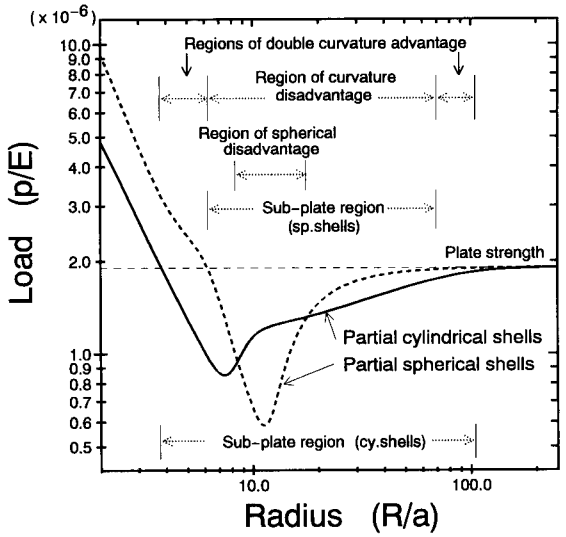

Fig.9 Comparison of the elastic strength characteristics between the two types of shells and the identification of different regions

in Fig. (8) since the order of tangential shear stresses are found to be much smaller to pose any serious threat of contributing to an initial limit stress state.

3.2.2 Strength Characteristics

Similar to the typical result shown in Fig. 8, the limit stresses for different curvatures are calculated and the results are summarized in Fig. 9 for the two types of shells. From these elastic strength characteristics a comparative study is made possible between the two shell types. The spherical shells are found to be more highly prone to reach an earlier strength limit for a particular range of curvatures than their cylindrical counterparts.

It is interesting to note that shells in a particular curvature range have their strength limits reached, although at a local monitoring point and not a global state, even before the corresponding value for a simple plate. This phenomenon at the first glance runs contrary to the popular idea of shells being stronger due to their form resistance. However, this analysis considers only the local stress limit and does not include any other considerations like the geometrical strength, stability, ultimate strength or global elastic/plastic limits. Also, there is a region where the addition of a curvature to the cylindrical shell could enhance its strength in par with that of spherical shells.

It might be concluded from Fig. 9 that for shallow shells, the simple plate is the upper limit in a local strength perspective, and the real manifestations of shell strength are visible mainly in the deep curvature ranges for both types of shells.

3.2.3 A Comparative Study of Shell Characteristics

The characteristics of resisting mechanisms and strength that were demonstrated separately are combined into one in Fig. 10 and Fig. 11, where the curves of strength limits for each shell are drawn along with the characteristic curves of resisting mechanisms. The 'extension only' zone of resisting mechanism can be found to be the same as the region of 'shell strength' determined by the strength analysis. Similarly, the 'bending only' zone is roughly the same as the 'equi-plate strength' zone. The most intricate among these zones, the 'extension and bending' zone, can be seen to indicate the 'sub-plate strength' zone, which explains the fact that any amount of lowering of the influence of bending stiffness also renders the shell strength to be

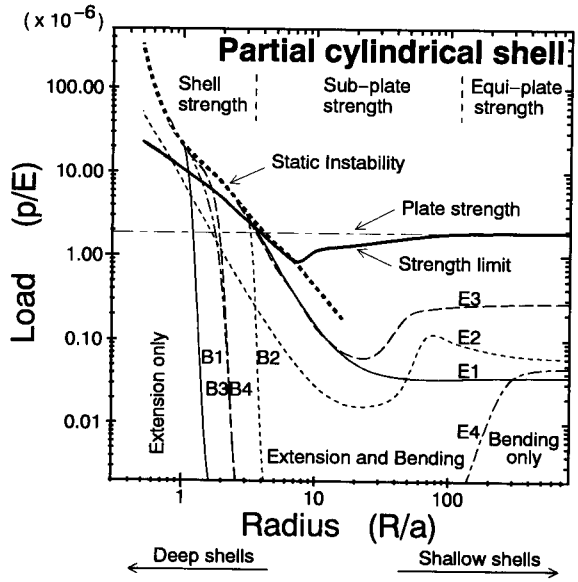

Fig.10 Comparison between the resisting mechanisms and elastic strength characteristics of partial cylindrical shells

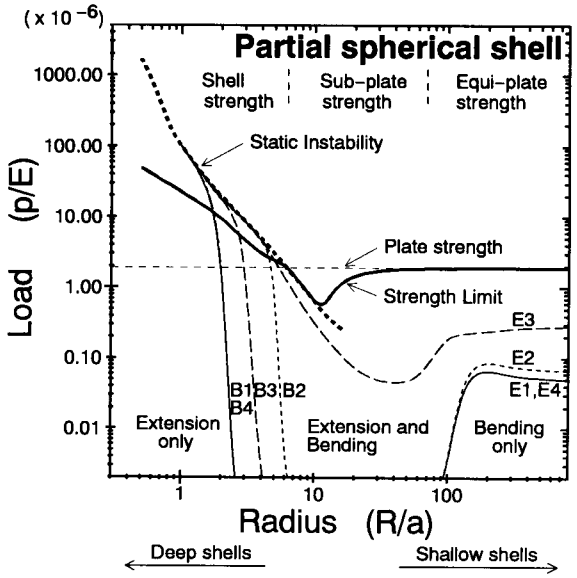

Fig.11 Comparison between the resisting mechanisms and elastic strength characteristics of partial spherical shells

'sub-plate' until the extensional stiffness regains the dominating status near to the 'extension only' zone, where the 'shell strength' is attained.

Based on the numerical evidence obtained in this research, a broad classification of shell curvatures become possible. In Fig. 12 the conclusions drawn from the analyses of resisting mechanisms are demonstrated at the top and bottom third of the figure along with the results of strength analyses shown in the middle portion. The top and bottom halves of the figure represent the cases of partial cylindrical and partial spherical shells respectively.

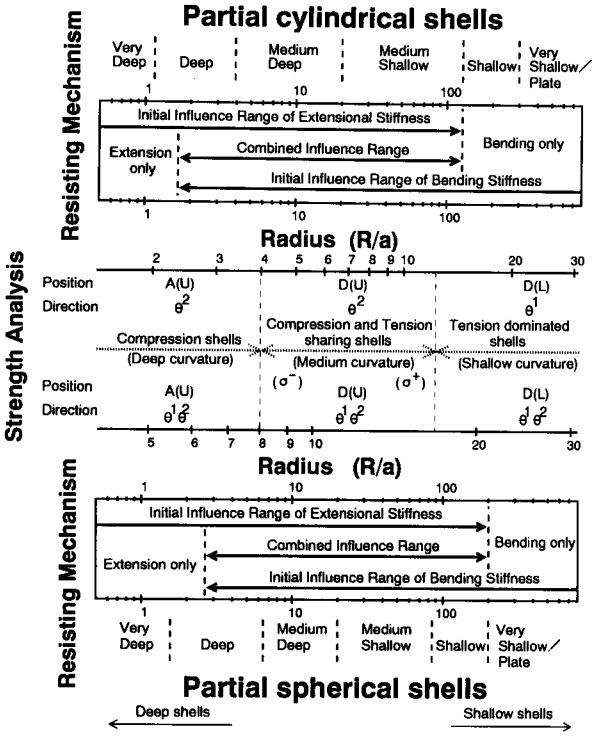

Fig.12 A depiction of qualitatively equi-strength curvature regions and their limiting strength specifications against the different regions of resisting mechanisms of the two types of shells

The terminology used here for the subdivision of curvatures and different ranges of mechanisms are arbitrary and self-explanatory. The upper and lower horizontal scales are staggered in the middle figure, where the strength analysis is shown, to facilitate direct comparisons between the equi-strength curvatures of the two types of shells. Also indicated in the middle figure are the monitoring positions and the principal directions of the initial limit stress state. The dominant stress states at the two ends of the medium curvature range [(σ^+) : tensile stress, (σ^-) : compressive stress] are also shown.

This subdivision is a qualitative depiction comparing the resisting mechanisms and strength characteristics of shells in a picto-verbal sense, which is considered suitable as a quick reference into the different shell mechanisms.

4. Conclusions

Some characteristics of thin shells with respect to their resisting mechanisms and strength have been brought out and the correlations between the two were graphically demonstrated through the numerical results presented in this paper. The resisting mecha-

nism was analyzed within the statically stable region and the strength was evaluated based on certain local elastic criteria. Both these aspects have shown that the medium range of curvatures, which has wide practical applications, is the most intricate area that act as a transition range between shallow and deep shells, where the problem has to be approached with extreme caution.

Obviously, any practical design criteria for shell structures have to take care of all these different aspects simultaneously. The present approach could be not applicable to the accompanying dynamic phenomena, if any, where some small nonlinearities at an initial stage could be a detrimental factor to the equilibrating mechanism. The results presented here for the particular shell types could serve as a useful guideline for other types of shell problems too.

References

1) Flügge, W.: Stresses in Shells, Springer-Verlag, Berlin (1960)
2) Green, A. E., Zerna, W.: Theoretical Elasticity, Oxford University Press, Oxford (1960)
3) Flügge, W.: Tensor Analysis and Continuum Mechanics, Springer-Verlag, New York (1972)
4) Pietraszkiewicz, W.: Geometrically Nonlinear Theories of Thin Elastic Shells, Advances in Mechanics, **12** (1989), pp. 51～130
5) Shinoda, T., George, T., Fukuchi, N.: A Detailed Analysis of the Theory of Thin Shells and some Particular Applications, Trans. of the West Japan Society of Naval Architects, No. 80 (1990), pp. 171～193
6) Fukuchi, N., George, T., Shinoda, T.: Dynamic Instability Analysis of Thin Shell Structures subjected to Follower Forces, (2 nd Report) Numerical Solutions and some Theoretical Concepts, Journal of the Society of Naval Architects of Japan, No. 171 (1992), pp. 597～609
7) George, T., Fukuchi, N.: Dynamic Instability Analysis of Thin Shell Structures subjected to Follower Forces, (6 th Report) Dynamic Threshold Characteristics and Post-critical Stability, Journal of the Society of Naval Architects of Japan, No. 176 (1994), pp. 319～330
8) George, T., Okada, H., Fukuchi, N.: The Resisting Mechanism during the Large Normal Deflection of Thin Shells subjected to Follower Forces, Journal of the Society of Naval Architects of Japan, No. 179 (1996), pp. 281～292